

Quantum Monte Carlo Study of a Positron in an Electron Gas: Auxiliary Material

N. D. Drummond

Department of Physics, Lancaster University, Lancaster LA1 4YB, United Kingdom

P. López Ríos and R. J. Needs

*TCM Group, Cavendish Laboratory, University of Cambridge,
J. J. Thomson Avenue, Cambridge CB3 0HE, United Kingdom*

C. J. Pickard

University College London, Gower Street, London WC1E 6BT, United Kingdom

(Dated: April 28, 2011)

I. ADDITIONAL PLOTS OF THE QUANTUM MONTE CARLO RESULTS

A. Relaxation energy

Figure 1 shows the relaxation energy $\Delta\Omega(r_s)$ of a positron in a homogeneous electron gas (HEG) from various calculations. It contains the same data as Fig. 1 of the main text together with the energies of Ps and Ps^- .

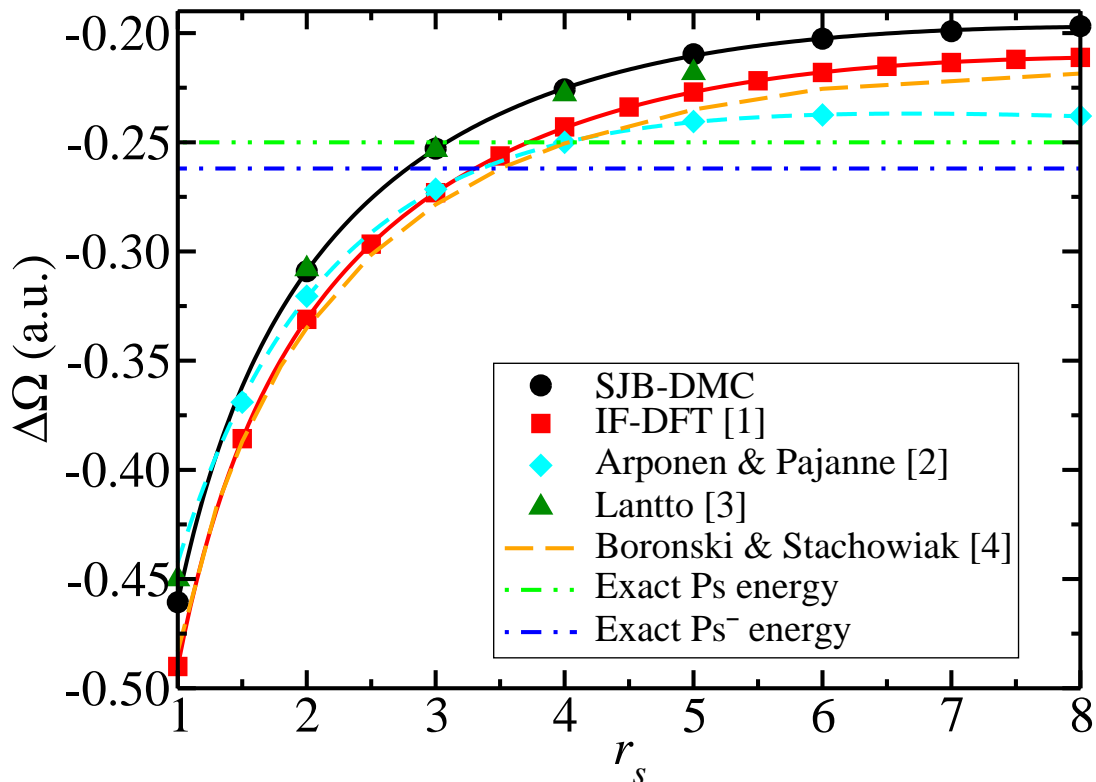


FIG. 1: Slater-Jastrow-backflow diffusion Monte Carlo (SJB-DMC) relaxation energy (electron-positron correlation energy) $\Delta\Omega$ against density parameter r_s , together with other results from the literature [1–4]. The exact energy of Ps^- is taken from Ref. 5. Wave-function form $\Psi_{\text{PW}}^{\text{SJB}}$ from Eq. (1) of the main text and $N = 54$ electrons were used in the SJB-DMC calculations.

B. Complete pair-correlation function

The full pair-correlation function (PCF) results are plotted in Fig. 2. There is good agreement between the Slater-Jastrow-backflow quantum Monte Carlo (SJB-QMC) and impurity-frame density functional theory (IF-DFT) results

at short range, but the agreement is less good at $r \simeq r_s$. The IF-DFT theory satisfies the electron-positron cusp condition, which is very important in obtaining accurate values of $g(0)$.

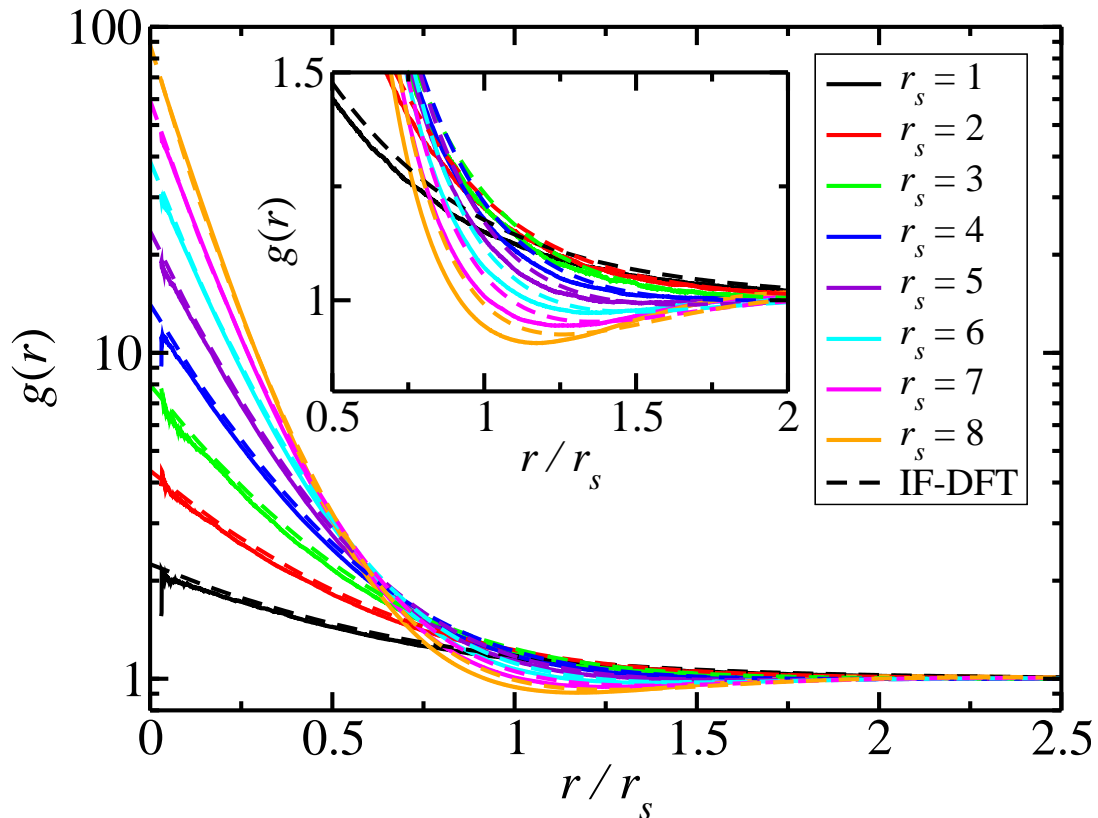


FIG. 2: Electron-positron PCFs, obtained by extrapolated estimation using DMC and variational Monte Carlo (VMC) calculations with wave-function form $\Psi_{\text{PW}}^{\text{SJB}}$ from Eq. (1) in the main text (solid curves). IF-DFT PCFs [1] are also shown (dashed curves). The QMC calculations were performed in cells with $N = 54$ electrons and the raw PCFs were multiplied by $N/(N-1)$ as discussed in Ref. 1. Some noise is visible in the QMC data at short range due to the small amount of data in this region. The inset shows the region $r \approx r_s$ in greater detail.

C. Contact pair-correlation-function data

Figure 3 shows the overall variation of the contact PCF $g(0)$ with r_s . The data of Apaja *et al.* [6] deviate strongly from the other data at large r_s , giving much larger values of $g(0)$. At large r_s , the fitting form used for the IF-DFT and SJB-DMC data tends to the limit appropriate for a Ps^- ion [1], whereas the Boroński-Nieminen form [4] tends to the limit appropriate for a Ps atom. As a result, the curves fitted to the IF-DFT and SJB-DMC data must ultimately exceed the Boroński-Nieminen formula (but at larger r_s than shown in Fig. 3 of the main body of our article).

II. LOW WEIGHT ABOVE THE FERMI MOMENTUM IN THE ANNIHILATING-PAIR MOMENTUM DENSITY

A. Cancellation of post-edge tails due to electron-electron and electron-positron correlation

Consider a positron immersed in a HEG. The dominant form of correlation in a positron-in-HEG system is described by the two-body $u(r)$ term in the Jastrow exponent: this term retrieves the bulk of the correlation energy. We therefore consider calculating the annihilating-pair momentum density (APMD) using a many-body wave function of the form $\Psi_{\text{PW}}^{\text{SJ}}$ in Eq. (1) of the main text, with only a two-body $u(r)$ term being present in the Jastrow exponent.

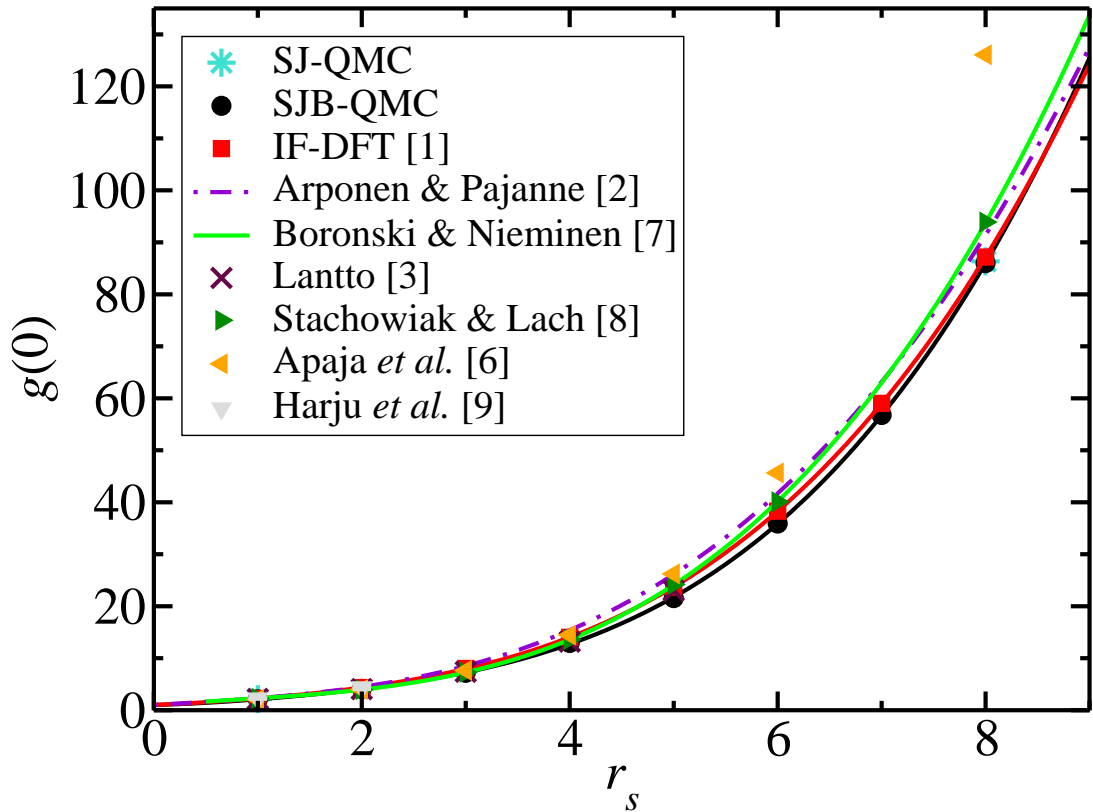


FIG. 3: Electron-positron contact PCF $g(0)$ against density parameter r_s from our QMC calculations, as calculated using extrapolated estimation from Slater-Jastrow VMC (SJ-VMC) and SJ-DMC calculations and from SJB-VMC and SJB-DMC calculations, and other studies [1–3, 6–9]. The extrapolated SJ-QMC and SJB-QMC results are in excellent agreement.

The long-range two-body Jastrow factor is determined by the random phase approximation (RPA). This shows that the long-range electron-positron two-body Jastrow exponent $u_{ep}(r)$ is [10]

$$u_{ep}(r) \approx 1/(\omega_p r) \approx -u_{\uparrow\downarrow}(r) \approx -u_{\uparrow\uparrow}(r), \quad (1)$$

where the long-range electron-electron two-body Jastrow factor is $u_{\uparrow\downarrow}(r)$ for antiparallel spins and $u_{\uparrow\uparrow}(r)$ for parallel spins, and $\omega_p = \sqrt{3/r_s^3}$ is the classical plasma frequency of the HEG. This relationship is exact in the limit of large r . (The RPA is linear response theory in the rest frame of one of the particles, which is regarded as an impurity. The response to an electron is equal and opposite to the response to a positron.)

The Kato cusp conditions [11] on the antiparallel-spin electron-electron and electron-positron two-body terms in the Jastrow exponent may be written as

$$\left(\frac{\partial u_{ep}}{\partial r}\right)_{r=0} = -\frac{1}{2} = -\left(\frac{\partial u_{\uparrow\uparrow}}{\partial r}\right)_{r=0}. \quad (2)$$

Constant offsets to the Jastrow exponent only change the normalization of the wave function. So, for all r , at both long range and short range, we expect that $u_{ep}(r) \approx -u_{\uparrow\downarrow}(r)$.

The parallel-spin Kato cusp condition differs from the antiparallel-spin cusp condition, and so $u_{\uparrow\uparrow}(r)$ must differ from $-u_{ep}(r)$ at short range. However, the overall wave function is small when two parallel-spin electrons are close, due to antisymmetry (the wave function goes to zero when the electrons coincide, even if the electron-positron distance is constrained to equal the electron-electron distance). So, for all r , either $u_{ep}(r) \approx -u_{\uparrow\uparrow}(r)$ or the wave function is small.

Hence an SJ wave function with the constraint $-u_{ep} = u_{\uparrow\downarrow} = u_{\uparrow\uparrow}$ (in which the electron-positron and antiparallel-spin electron-electron Kato cusp conditions are satisfied) can be expected to be a good approximation to the ground-state wave function. The energy data presented in Tables I and II show that this is indeed the case. We may write

this wave function as

$$\Psi_{\text{PW}}^{\text{SJC}}(\mathbf{r}_p; \mathbf{r}_1, \dots, \mathbf{r}_N) = \exp \left[\sum_{i=1}^N u_{\text{ep}}(|\mathbf{r}_i - \mathbf{r}_p|) + \sum_{i=1}^{N_\uparrow-1} \sum_{j=i+1}^{N_\uparrow} u_{\uparrow\uparrow}(|\mathbf{r}_i - \mathbf{r}_j|) \right. \\ \left. + \sum_{i=N_\uparrow+1}^{N-1} \sum_{j=i+1}^N u_{\uparrow\uparrow}(|\mathbf{r}_i - \mathbf{r}_j|) + \sum_{i=1}^{N_\uparrow} \sum_{j=N_\uparrow+1}^N u_{\uparrow\downarrow}(|\mathbf{r}_i - \mathbf{r}_j|) \right] S(\mathbf{r}_1, \dots, \mathbf{r}_N), \quad (3)$$

where there are $N = N_\uparrow + N_\downarrow$ electrons in total, the first N_\uparrow being spin-up. \mathbf{r}_i is the position of electron i and \mathbf{r}_p is the position of the positron. S is the Slater wave function, which is a product of determinants of plane-wave orbitals for spin-up and spin-down electrons. The wave function when the positron coincides with electron 1 at position \mathbf{r}_1 is

$$\Psi_{\text{PW}}^{\text{SJC}}(\mathbf{r}_1; \mathbf{r}_1, \dots, \mathbf{r}_N) = \exp \left[\sum_{i=2}^{N_\uparrow-1} \sum_{j=i+1}^{N_\uparrow} u_{\uparrow\uparrow}(|\mathbf{r}_i - \mathbf{r}_j|) + \sum_{i=N_\uparrow+1}^{N-1} \sum_{j=i+1}^N u_{\uparrow\uparrow}(|\mathbf{r}_i - \mathbf{r}_j|) \right. \\ \left. + \sum_{i=2}^{N_\uparrow} \sum_{j=N_\uparrow+1}^N u_{\uparrow\downarrow}(|\mathbf{r}_i - \mathbf{r}_j|) \right] S(\mathbf{r}_1, \dots, \mathbf{r}_N). \quad (4)$$

So the electron-electron and electron-positron two-body terms cancel out of the Jastrow exponent, which therefore does not depend on \mathbf{r}_1 . Take the Fourier transform with respect to \mathbf{r}_1 to obtain the electron-positron center-of-mass momentum wave function

$$\Psi_{\text{PW}}^{\text{SJC}}(\bar{\mathbf{p}}_1, \mathbf{r}_2, \dots, \mathbf{r}_N) = \exp \left[\sum_{i=2}^{N_\uparrow-1} \sum_{j=i+1}^{N_\uparrow} u_{\uparrow\uparrow}(|\mathbf{r}_i - \mathbf{r}_j|) + \sum_{i=N_\uparrow+1}^{N-1} \sum_{j=i+1}^N u_{\uparrow\uparrow}(|\mathbf{r}_i - \mathbf{r}_j|) \right. \\ \left. + \sum_{i=2}^{N_\uparrow} \sum_{j=N_\uparrow+1}^N u_{\uparrow\downarrow}(|\mathbf{r}_i - \mathbf{r}_j|) \right] \int S(\mathbf{r}_1, \dots, \mathbf{r}_N) \exp(-i\bar{\mathbf{p}}_1 \cdot \mathbf{r}_1) d\mathbf{r}_1. \quad (5)$$

Expanding the Slater determinants S as a sum of products of plane-wave orbitals, it is clear that if $\bar{\mathbf{p}}_1$ corresponds to an unoccupied \mathbf{k} vector then,

$$\int S(\mathbf{r}_1, \dots, \mathbf{r}_N) \exp(-i\bar{\mathbf{p}}_1 \cdot \mathbf{r}_1) d\mathbf{r}_1 = 0. \quad (6)$$

In the infinite-system limit we therefore have $\Psi_{\text{PW}}^{\text{SJC}}(\bar{\mathbf{p}}_1, \mathbf{r}_2, \dots, \mathbf{r}_N) = 0$ for $|\bar{\mathbf{p}}_1| > k_F$, where k_F is the Fermi momentum. The APMD is

$$\rho_{\text{PW}}^{\text{SJC}}(\bar{\mathbf{p}}) \propto \int \dots \int |\Psi_{\text{PW}}^{\text{SJC}}(\bar{\mathbf{p}}, \mathbf{r}_2, \dots, \mathbf{r}_N)|^2 d\mathbf{r}_2 \dots d\mathbf{r}_N. \quad (7)$$

So $\rho_{\text{PW}}^{\text{SJC}}(\bar{\mathbf{p}}) = 0$ for $|\bar{\mathbf{p}}| > k_F$.

The $\Psi_{\text{PW}}^{\text{SJC}}$ wave-function form is only an approximation to the exact ground-state wave function, and hence the conclusion of the above argument can only be expected to hold approximately for the true wave function.

B. Test calculations with constrained Jastrow exponents

The argument given in Sec. II A hinges on the fact that $u_{\uparrow\downarrow}(r) \approx u_{\uparrow\uparrow}(r) \approx -u_{\text{ep}}(r)$, which is Eq. (3) of the main text. To illustrate the degree to which this condition is obeyed, we plot the various Jastrow exponents obtained from a VMC optimization at $r_s = 8$ in Fig. 4 with 54 electrons. We used two-body Jastrow exponents consisting of a spherically symmetric term and an expansion in plane waves [12]. The Jastrow factor is not quite spherically symmetric because of the plane-wave term, but the best possible two-body Jastrow exponent would not be exactly spherically symmetric either, because of the use of a finite simulation cell. In Fig. 4 we plot the total Jastrow exponent along the x -axis in a cubic unit cell. For clarity of presentation, the Jastrow exponents have been offset so that they are equal at $r = 2.9r_s$, which is the radius of the largest sphere enclosed by the Wigner-Seitz cell of the simulation

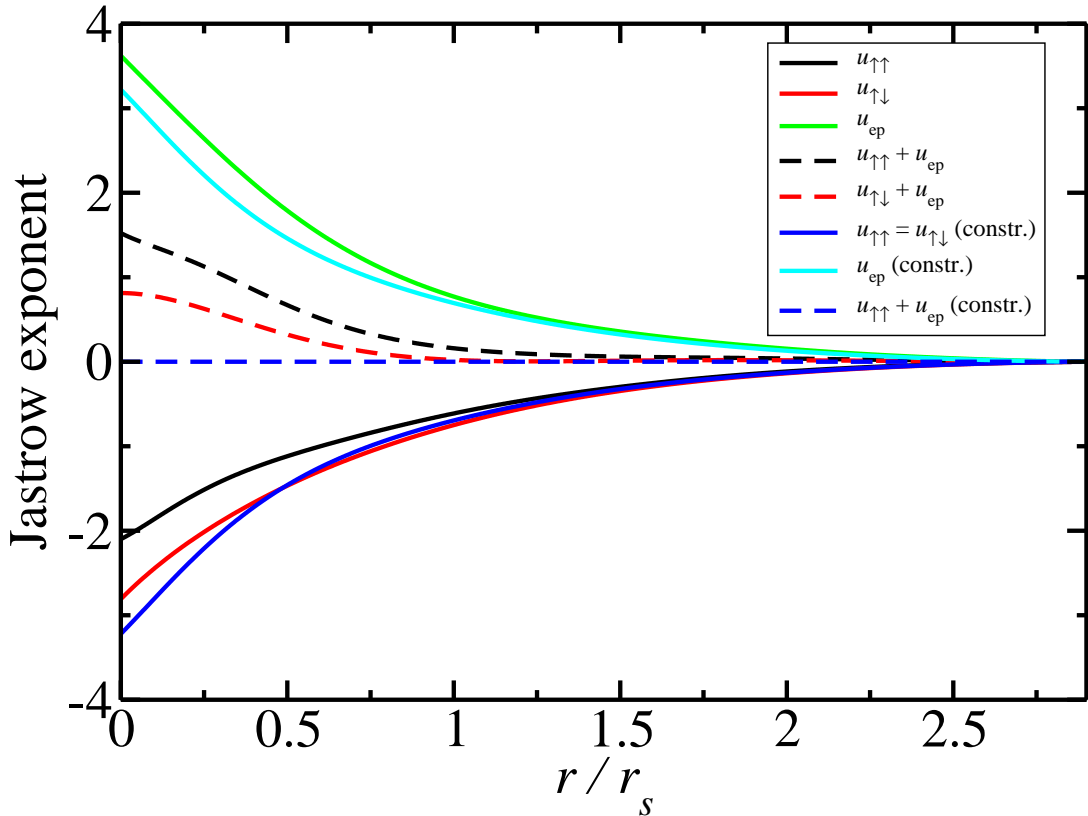


FIG. 4: Variation of the two-body Jastrow exponents with particle separation in the x -direction for a positron in a HEG of density $r_s = 8$ with 54 electrons in a cubic cell. The Jastrow exponents were optimized within VMC. The Jastrow exponents have been offset so that they are identical at $r = 2.9r_s$, which is the radius of the largest sphere enclosed by the Wigner-Seitz cell of the simulation cell.

cell. These offsets have no effect on the numerical results obtained, since they only affect the normalization of the wave function.

It can be seen that $u_{\uparrow\downarrow}(r) \simeq -u_{\text{ep}}(r)$ with only small deviations at small r . Although $u_{\uparrow\uparrow}(r)$ deviates from $-u_{\text{ep}}(r)$ at distances less than about r_s , the probability of parallel-spin electrons being at a separation less than r_s is small, due to antisymmetry. This confirms the validity of our argument. It is also demonstrated in Tables I and II that imposing Eq. (3) of the main text (satisfying the electron-positron and antiparallel-spin cusp conditions, but violating the less-important parallel-spin cusp condition) gives reasonable energies and variances (although these are significantly higher than the results obtained without the imposition of this constraint).

III. ADDITIONAL TECHNICAL DETAILS OF THE QMC CALCULATIONS

A. DMC time step and target population

For the positron-in-HEG DMC calculations the time steps were all in the range 0.01–0.05 a.u. For the HEG, larger time steps were used at large r_s , up to 0.2 a.u. at $r_s = 8$. The energies were extrapolated linearly to zero time step in each case. For the PCF, the statistical noise was much greater than the time-step bias, and so the DMC data at different time steps were averaged (weighted by the amount of data gathered).

In each DMC calculation the target population of walkers was 1024. We verified that the DMC energy of the positron-in-HEG system was converged with respect to the target population.

Method	WF	E_{cut} (a.u.)	p present	u constr.	Total energy (a.u.)	Variance (a.u.)
VMC	$\Psi_{\text{pair}}^{\text{SJ}}$	5	F	F	28.8758(4)	1.898
VMC	$\Psi_{\text{PW}}^{\text{SJ}}$	N/A	T	T	28.8680(4)	1.314
VMC	$\Psi_{\text{pair}}^{\text{SJ}}$	50	F	F	28.8670(5)	1.808
VMC	$\Psi_{\text{pair}}^{\text{SJ}}$	200	F	F	28.8639(7)	1.775
VMC	$\Psi_{\text{PW}}^{\text{SJ}}$	N/A	T	F	28.8176(3)	0.871
VMC	$\Psi_{\text{pair}}^{\text{SJ}}$	200	T	F	28.8105(2)	0.854
VMC	$\Psi_{\text{pair}}^{\text{SJB}}$	5	F	F	28.7692(6)	1.187
VMC	$\Psi_{\text{pair}}^{\text{SJB}}$	200	F	F	28.7639(7)	1.182
VMC	$\Psi_{\text{pair}}^{\text{SJB}}$	50	F	F	28.7638(5)	1.159
VMC	$\Psi_{\text{pair}}^{\text{SJB}}$	5	T	F	28.7164(6)	0.339
VMC	$\Psi_{\text{PW}}^{\text{SJB}}$	N/A	T	F	28.7109(3)	0.293
VMC	$\Psi_{\text{pair}}^{\text{SJB}}$	200	T	F	28.7098(3)	0.318
DMC	$\Psi_{\text{PW}}^{\text{SJ}}$	N/A	T	F	28.7662(2)	N/A
DMC	$\Psi_{\text{pair}}^{\text{SJ}}$	5	F	F	28.766(2)	N/A
DMC	$\Psi_{\text{pair}}^{\text{SJ}}$	200	T	F	28.7609(3)	N/A
DMC	$\Psi_{\text{pair}}^{\text{SJB}}$	5	F	F	28.7077(7)	N/A
DMC	$\Psi_{\text{pair}}^{\text{SJB}}$	50	F	F	28.7037(8)	N/A
DMC	$\Psi_{\text{PW}}^{\text{SJB}}$	N/A	T	F	28.7010(4)	N/A
DMC	$\Psi_{\text{pair}}^{\text{SJB}}$	200	T	F	28.6997(3)	N/A

TABLE I: Total energy and variance of energy for a 54-electron positron-in-HEG system at $r_s = 1$ a.u. The DMC results have been extrapolated to zero time step. The results were obtained using different wave functions (WFs) from Eq. (1) of the main text, plane-wave cutoff energies E_{cut} for the pairing orbitals, with and without a plane-wave two-body (p) term in the Jastrow factor, and with and without Eq. (3) of the main text being imposed on the two-body term u in the Jastrow exponent.

B. Choice of trial wave function and system size

1. Total energy

In this section we compare the QMC results obtained with the four wave-function forms $\Psi_{\text{PW}}^{\text{SJ}}$, $\Psi_{\text{PW}}^{\text{SJB}}$, $\Psi_{\text{pair}}^{\text{SJ}}$, and $\Psi_{\text{pair}}^{\text{SJB}}$ listed in Eq. (1) of the main text.

Total energies evaluated using VMC and DMC with different trial wave functions for a positron in a 54-electron HEG at $r_s = 1$ and $r_s = 8$ are shown in Tables I and II, respectively. It can be seen that backflow lowers the VMC and DMC energies significantly. A plane-wave two-body term in the Jastrow factor lowers the VMC energy even further. It even lowers the DMC energy very slightly (via its effect on the backflow function, which is optimized simultaneously), and makes the DMC calculation much more efficient. The dependence of the VMC and DMC energies on the plane-wave cutoff for the orbitals is relatively weak, especially if the Jastrow factor is used to impose the electron-positron cusp condition. At the DMC level with an SJB wave function, plane-wave and pairing orbitals give similar energies. At the VMC level, or if an SJ wave function is used, the pairing orbitals give lower QMC energies. The variance is substantially higher when pairing orbitals are used, however, presumably due to the noise introduced by the incomplete basis set.

DMC with wave function $\Psi_{\text{PW}}^{\text{SJB}}$ is substantially cheaper than DMC with wave function $\Psi_{\text{pair}}^{\text{SJB}}$ and gives similar energy results, so we have used wave function $\Psi_{\text{PW}}^{\text{SJB}}$ in our production DMC calculations. For the APMD, which is evaluated using VMC, we have used wave function $\Psi_{\text{pair}}^{\text{SJB}}$, since this gives the lowest VMC energy. Trial wave functions $\Psi_{\text{PW}}^{\text{SJB}}$ and $\Psi_{\text{pair}}^{\text{SJB}}$ contained 108 optimizable parameters for the positron-in-HEG calculations and the corresponding SJB wave function for the HEG contained 72 optimizable parameters.

2. Relaxation energy

As is usually the case in QMC studies of models of condensed matter, finite-size errors are the largest source of bias in our energy data. DMC relaxation energies obtained using four different wave functions together with IF-DFT relaxation energies against system size are plotted in Fig. 5. For $N < 54$ electrons there is a systematic bias due to

Method	WF	E_{cut} (a.u.)	p present	u constr.	Total energy (a.u.)	Variance (a.u.)
VMC	$\Psi_{\text{PW}}^{\text{SJ}}$	N/A	T	T	-3.53533(6)	0.01889
VMC	$\Psi_{\text{pair}}^{\text{SJ}}$	5	F	F	-3.55942(7)	0.01995
VMC	$\Psi_{\text{PW}}^{\text{SJB}}$	N/A	T	F	-3.56057(3)	0.01466
VMC	$\Psi_{\text{pair}}^{\text{SJB}}$	5	F	F	-3.56086(9)	0.03333
VMC	$\Psi_{\text{pair}}^{\text{SJ}}$	5	T	F	-3.56901(5)	0.01681
VMC	$\Psi_{\text{pair}}^{\text{SJB}}$	10	T	F	-3.56915(6)	0.01515
VMC	$\Psi_{\text{PW}}^{\text{SJB}}$	N/A	T	F	-3.587811(9)	0.01231
VMC	$\Psi_{\text{pair}}^{\text{SJB}}$	10	T	F	-3.5903(1)	0.02589
VMC	$\Psi_{\text{pair}}^{\text{SJB}}$	5	T	F	-3.5923(1)	0.01863
DMC	$\Psi_{\text{PW}}^{\text{SJ}}$	N/A	T	F	-3.5998(6)	N/A
DMC	$\Psi_{\text{pair}}^{\text{SJ}}$	10	T	F	-3.6009(3)	N/A
DMC	$\Psi_{\text{pair}}^{\text{SJ}}$	5	F	F	-3.6013(3)	N/A
DMC	$\Psi_{\text{pair}}^{\text{SJB}}$	5	F	F	-3.6105(5)	N/A
DMC	$\Psi_{\text{pair}}^{\text{SJB}}$	10	T	F	-3.6107(2)	N/A
DMC	$\Psi_{\text{PW}}^{\text{SJB}}$	N/A	T	F	-3.6112(2)	N/A
DMC	$\Psi_{\text{pair}}^{\text{SJB}}$	5	T	F	-3.6114(2)	N/A

TABLE II: Like Table II, but for a positron in a HEG at density parameter $r_s = 8$.

the interaction of images of the positron which can be (partially) corrected using the IF-DFT data, but for $N \geq 54$ the energies obtained at different system sizes oscillate in a quasi-random fashion. The oscillations correlate with the oscillations in the IF-DFT data, suggesting they are caused by single-particle finite-size errors, but the amplitude is much smaller for the DMC calculations. We therefore simply report our DMC results obtained with $N = 54$ electrons, without applying a finite-size correction. The uncertainty in the DMC relaxation energy due to finite-size errors ranges from about ± 0.003 a.u. at $r_s = 1$ to ± 0.001 a.u. at $r_s = 8$.

As can be seen in Fig. 5, the DMC relaxation energy depends only weakly on the choice of wave-function form ($\Psi_{\text{PW}}^{\text{SJ}}$, $\Psi_{\text{PW}}^{\text{SJB}}$, $\Psi_{\text{pair}}^{\text{SJ}}$, or $\Psi_{\text{pair}}^{\text{SJB}}$). The only exception is for the large $N = 114$ calculation at $r_s = 8$ using wave function $\Psi_{\text{pair}}^{\text{SJB}}$, where it was necessary to economize on the plane-wave cutoff energy because of limitations on the available memory. There is no obvious systematic trend or evidence that the SJB relaxation energies are better than the SJ relaxation energies (even though the energies of the positron-in-HEG and HEG are substantially lower when backflow is used, as shown in Tables I and II). We used wave-function form $\Psi_{\text{PW}}^{\text{SJB}}$ in our final DMC calculations.

3. APMD

VMC APMDs obtained with different trial wave functions and numbers of electrons are plotted in Fig. 6. It is clear that the APMD is very much more difficult to calculate with quantitative accuracy than the relaxation energy or the PCF: small changes to the trial wave function that have a negligible effect on the energy can have a large effect on the APMD. There is a substantial disagreement between the SJ and SJB results. The latter give a lower VMC energy and should therefore be more accurate. Likewise, there is a disagreement between the results obtained with plane-wave and pairing orbitals. The pairing orbitals give lower VMC energies, so we expect them to be more accurate. Furthermore the APMDs obtained with pairing orbitals at different system sizes are in better agreement with each other than the APMDs obtained with plane-wave orbitals. This may reflect the fact that there is less reliance on VMC wave-function optimization when pairing orbitals are used. We have therefore used wave function $\Psi_{\text{pair}}^{\text{SJB}}$ in our final APMD calculations.

Given the lack of system-size dependence in IF-DFT APMDs [1] and the substantial wave-function dependence in the VMC results, it is likely that the differences seen in Fig. 6 between the APMDs obtained at different system sizes for $N \geq 114$ is primarily due to differences in the wave functions resulting from the stochastic nature of the optimization process using a finite number of configurations. Our final QMC results for the APMD were obtained using VMC with $N = 114$ electrons.

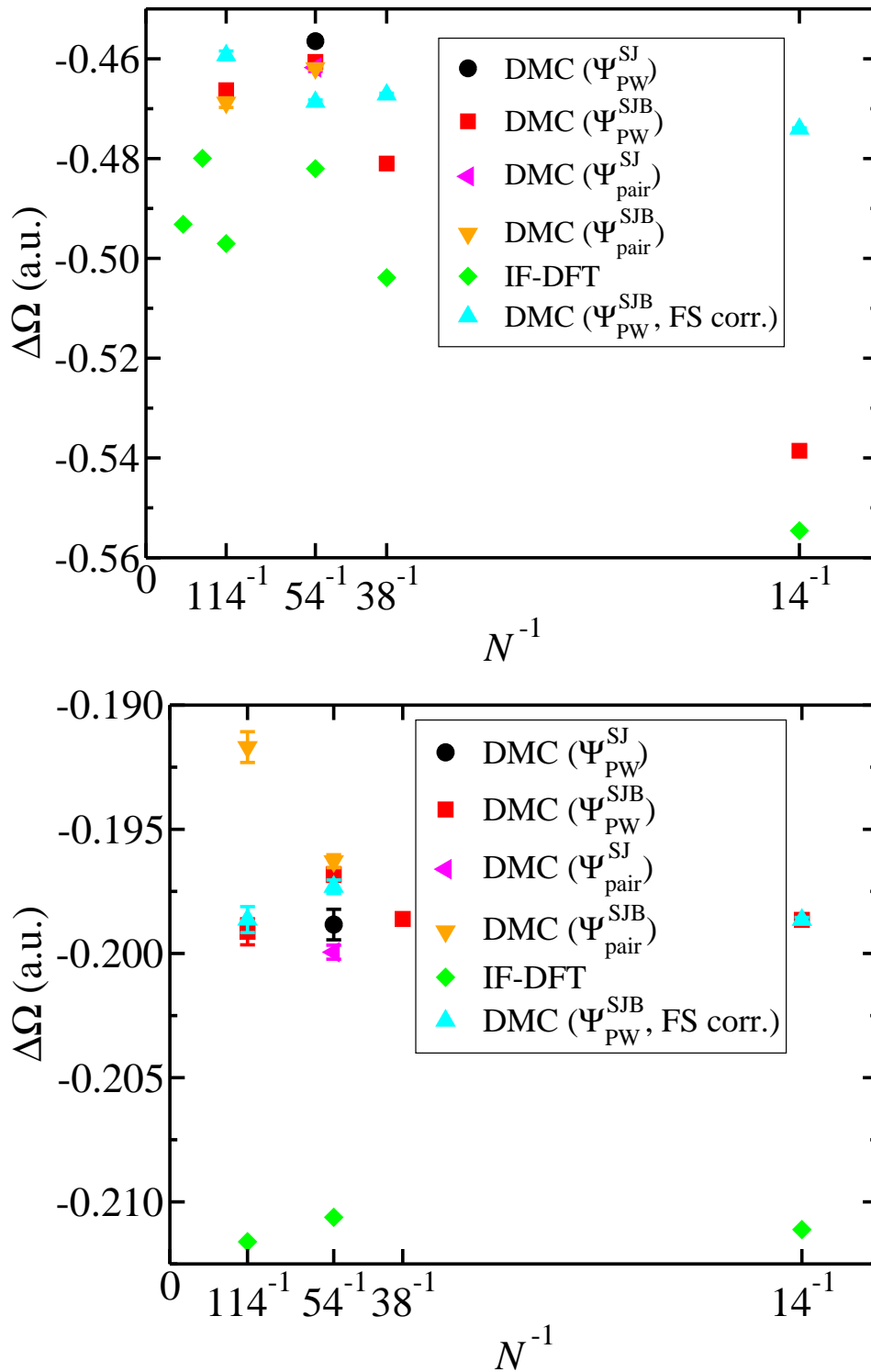


FIG. 5: Relaxation energy against system size at $r_s = 1$ (top panel) and $r_s = 8$ (bottom panel). The data labeled “FS corr.” have been finite-size corrected using the IF-DFT data.

4. PCF

As can be seen in Fig. 7, the contact PCFs obtained by extrapolated estimation using different wave-function forms are in good agreement, implying that the extrapolation process is successful. Despite the fact that the VMC and

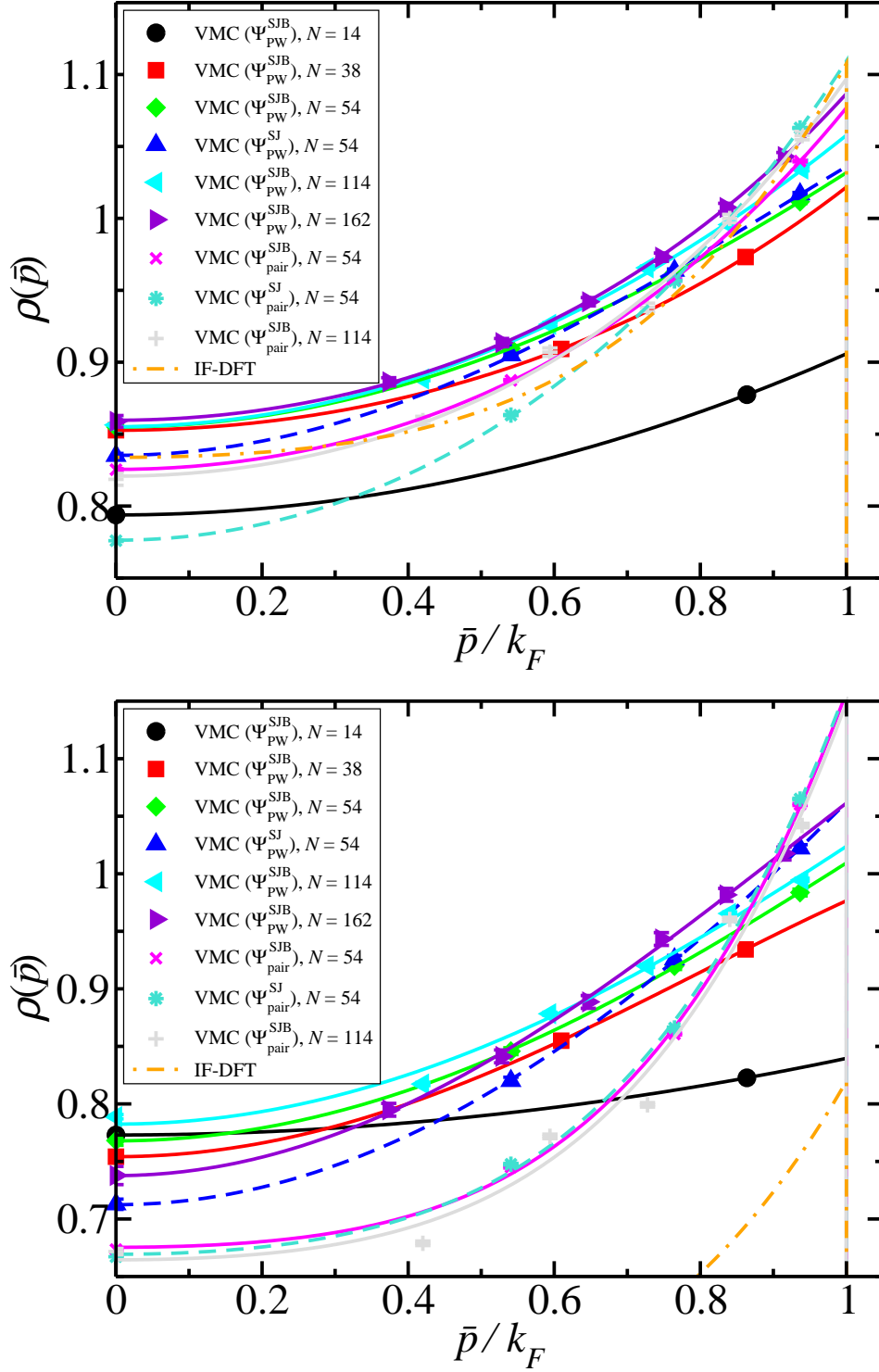


FIG. 6: APMD as calculated using VMC with different trial wave functions and different system sizes at $r_s = 1$ (top panel) and $r_s = 8$ (bottom panel). The IF-DFT APMD is also plotted in each case.

DMC energies are closer when the IF-DFT pairing orbitals are used (as shown in Tables I and II), there is no evidence that extrapolated estimation using the pairing orbitals is more accurate.

At low density the effects of extrapolated estimation are substantial, as can be seen in Table III. At high density ($r_s = 1$), however, the difference between the VMC and DMC results is not statistically significant.

Extrapolated estimates of the contact PCF obtained using different wave functions are plotted against system size

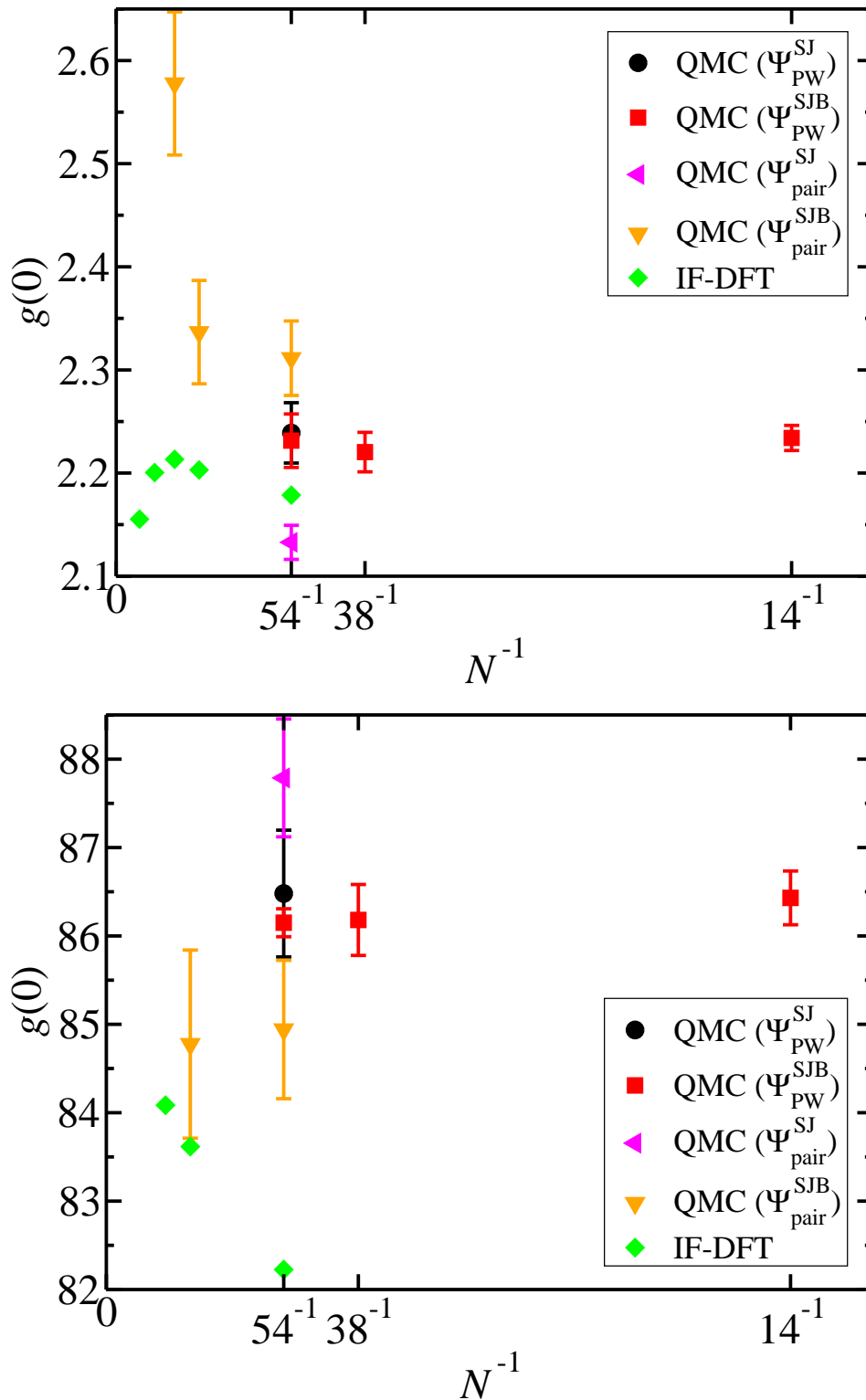


FIG. 7: Electron-positron contact PCF $g(0)$ against system size at $r_s = 1$ (top panel) and $r_s = 8$ (bottom panel). The QMC data were obtained by extrapolated estimation. The PCF data have been multiplied by $N/(N - 1)$ as discussed in Ref. 1.

in Fig. 7. The uncertainty arising from the choice of wave-function form appears to be larger than the uncertainty due to finite-size errors. Our final results were obtained using wave function Ψ_{PW}^{SJB} and $N = 54$ electrons. The overall uncertainty in our $g(0)$ data ranges from ± 0.05 at $r_s = 1$ to ± 0.5 at $r_s = 8$.

Method	WF	$g(0)$
VMC	$\Psi_{\text{PW}}^{\text{SJ}}$	64.4(4)
DMC	$\Psi_{\text{PW}}^{\text{SJ}}$	76.1(2)
Extrap.	$\Psi_{\text{PW}}^{\text{SJ}}$	86.3(5)
VMC	$\Psi_{\text{PW}}^{\text{SJB}}$	68.3(1)
DMC	$\Psi_{\text{PW}}^{\text{SJB}}$	77.07(7)
Extrap.	$\Psi_{\text{PW}}^{\text{SJB}}$	86.0(1)
VMC	$\Psi_{\text{pair}}^{\text{SJ}}$	71.1(3)
DMC	$\Psi_{\text{pair}}^{\text{SJ}}$	79.2(1)
Extrap.	$\Psi_{\text{pair}}^{\text{SJ}}$	87.6(4)
VMC	$\Psi_{\text{pair}}^{\text{SJB}}$	79.3(5)
DMC	$\Psi_{\text{pair}}^{\text{SJB}}$	81.6(1)
Extrap.	$\Psi_{\text{pair}}^{\text{SJB}}$	83.9(5)

TABLE III: Contact PCF for a positron immersed in a 54-electron HEG at $r_s = 8$ using different methods and wave functions (WFs).

C. Procedure for obtaining the contact PCF

Our PCFs were obtained by binning the electron-positron distances sampled in the course of the QMC simulations. Determining the contact PCF is difficult because this region is sampled infrequently, resulting in poor statistics. We have tried to minimize the effects of noise in the PCF data by extrapolating the $g(r)$ results obtained at finite r to $r = 0$.

For the DMC $g(0)$ data, time step errors are negligible compared with the statistical errors. We therefore averaged over the DMC data at different time steps weighted by the length of the simulation in imaginary time. The extrapolated PCF was then evaluated as $g_{\text{ext}}(r) = 2g_{\text{DMC}}(r) - g_{\text{VMC}}(r)$, where g_{DMC} and g_{VMC} are the DMC and VMC estimates of $g(r)$, respectively. The PCF data were then multiplied by $N/(N-1)$ to make the PCF tend to 1 at long range, as discussed in Ref. 1. We then fitted the polynomial $a_0 - r + a_2 r^2 + a_3 r^3$ to $\log[g(r)]$ on $0 < r < r_s/2$, where a_0 , a_2 , and a_3 are fitting parameters. This polynomial satisfies the Kimball cusp conditions [13]. Our estimate of the contact PCF is $g(0) = \exp(a_0)$.

In order to determine the error bars on $g(0)$, we assigned uniform error bars to the binned $g(r)$ data such that the χ^2 value of the fit was equal to the number of data. Hence we could determine the standard error in $g(0) = \exp(a_0)$.

D. Calculating the APMD

The APMD is calculated within VMC by performing an N -particle VMC calculation in which the wave function is $\Psi(\mathbf{r}_1; \mathbf{r}_1, \dots, \mathbf{r}_N)$, where $\Psi(\mathbf{s}; \mathbf{r}_1, \dots, \mathbf{r}_N)$ is the wave function for the positron-in-HEG system. The APMD is evaluated as

$$\rho(\bar{\mathbf{p}}) = \left\langle \frac{1}{(2\pi)^3} \int \frac{\Psi(\mathbf{r}; \mathbf{r}, \mathbf{r}_2, \dots, \mathbf{r}_N)}{\Psi(\mathbf{r}_1; \mathbf{r}_1, \dots, \mathbf{r}_N)} \exp[i\bar{\mathbf{p}} \cdot (\mathbf{r}_1 - \mathbf{r})] d\mathbf{r} \right\rangle, \quad (8)$$

where the angled brackets denote an average over the set of electron configurations generated by the VMC algorithm, which are distributed as $|\Psi|^2$. The integral in the expectation value of Eq. (8) is estimated by Monte Carlo sampling at each configuration generated by the VMC algorithm, and the results are averaged. The use of a finite number of points in the evaluation of the integral does not bias the estimate of $\rho(\bar{\mathbf{p}})$.

-
- [1] N.D. Drummond, P. López Ríos, C.J. Pickard, and R.J. Needs, Phys. Rev. B **82**, 035107 (2010).
[2] J. Arponen and E. Pajanne, Ann. Phys. **121**, 343 (1979).
[3] L.J. Lantto, Phys. Rev. B **36**, 5160 (1987).
[4] E. Boroński and H. Stachowiak, Phys. Rev. B **57**, 6215 (1998).
[5] A.M. Frolov, Phys. Lett. A **342**, 430 (2005).
[6] V. Apaja, S. Denk, and E. Krotscheck, Phys. Rev. B **68**, 195118 (2003).

- [7] E. Boroński and R.M. Nieminen, Phys. Rev. B **34**, 3820 (1986).
- [8] H. Stachowiak and J. Lach, Phys. Rev. B **48**, 9828 (1993).
- [9] A. Harju, B. Barbiellini, S. Siljamäki, R.M. Nieminen, and G. Ortiz, J. Radioanal. Nucl. Chem. **211**, 193 (1996).
- [10] T. Gaskell, Proc. Phys. Soc. **77**, 1182 (1961).
- [11] T. Kato, Commun. Pure Appl. Math. **10**, 151 (1957); R.T. Pack and W.B. Brown, J. Chem. Phys. **45**, 556 (1966).
- [12] N.D. Drummond, M.D. Towler, and R.J. Needs, Phys. Rev. B **70**, 235119 (2004).
- [13] J.C. Kimball, Phys. Rev. A **7**, 1648 (1973).